Research on Engineering Structures & Materials
www.jresm.org
Research Group

Research Article

Evaluation of CFRP confinement performance and predictive accuracy of design codes and stress-strain models for concrete

Abdellah Douadi[*,1,a], Riad Babba[2,b], Kamel Hebbache[1,c], Mourad Boutlikht[1,d], Nour El Houda Khitas[1,e], Abderraouf Messai[1,f], Redha Hammouche[3,g]

[1]*Civil Eng. Research Laboratory of Setif (LRGCS), Dept. of Civil Eng., Ferhat Abbas University of Setif 1, Algeria*
[2]*Faculty of Science and Technology, University of Tamanghasset, Algeria*
[3]*Materials and Durability of Construction Laboratory, Dept. of Civil Eng., Faculty of Science and Technology, Frères Mentouri University of Constantine 1, Algeria*

Article Info

Article history:

Received 06 Sep 2024
Accepted 05 Nov 2024

Keywords:

CFRP confinement;
Stress-strain models;
Design codes;
Concrete reinforcement

Abstract

This research investigates the effectiveness of different CFRP confinement types full, horizontal, and spiral and assesses the accuracy of various design codes and stress-strain models in predicting the performance of CFRP-confined concrete. Experimental results show that fully CFRP-confined specimens exhibit a significant increase in compressive strength by 89.36% compared to unconfined concrete, which had a compressive strength of 21.42 MPa, while horizontal CFRP strips with 30 mm spacing provide notable improvements in both strength (49.53% increase) and axial strain (610.78% increase). In contrast, spiral CFRP strips demonstrated lower effectiveness. Numerical evaluations revealed that the FIB model was accurate for horizontal confinements but overestimated compressive strength for spiral confinements. The ACI code offered reasonable predictions with deviations between -16% and 19%. Pellegrino et al and Wang et al. models performed well for horizontal CFRP strips but were less accurate for spiral configurations. The model proposed by Guo et al. overestimated the compressive strength for partially confined specimens. This study provides insights for optimizing CFRP confinement strategies and highlights the need for refinement in predictive models and design codes.

1. Introduction

Civil engineers frequently confront the critical task of maintaining and rehabilitating existing concrete structures that have sustained damage due to material degradation, natural disasters, or inherent design deficiencies [1]. The need to enhance the durability and load-bearing capacity of such structures has led to the increasing adoption of fiber-reinforced polymers (FRPs) as reinforcement materials. FRPs, characterized by their exceptional strength-to-weight ratio, high corrosion resistance [2, 3], and outstanding ductility, have demonstrated significant potential in extending the service life of concrete structures, particularly under adverse environmental conditions and loadings [3, 4].

The damage caused by earthquakes, particularly in reinforced concrete structures, has further emphasized the urgent need for reinforcement, especially in buildings constructed with low-strength concrete [5, 6]. Earthquakes generate significant lateral and vertical forces that can severely compromise the structural integrity of these structures, leading to cracking, spalling, and even catastrophic collapses [7, 8]. The devastating 2023 Turkey-

[*]Corresponding author: abdellah.douadi@univ-setif.dz
[a]orcid.org/0000-0002-7761-8488; [b]orcid.org/0000-0001-8742-1403; [c]orcid.org/0000-0002-4409-3689; [d]orcid.org/0000-0003-0808-6438; [e]orcid.org/0009-0002-8854-4266; [f]orcid.org/0000-0002-5769-2218; [g]orcid.org/0009-0004-4458-8309
DOI: http://dx.doi.org/10.17515/resm2024.435me0906rs

Syria earthquake serves as a stark reminder of the consequences of inadequate reinforcement and the use of substandard materials, which contributed to widespread destruction and tragic loss of life [9]. Reinforcing low-strength concrete structures is essential for improving their ductility, energy dissipation, and overall resilience to seismic loads [10]. This need for reinforcement arises from concrete's inherent limitations, as it is strong in compression but weak in tension and shear. To overcome these weaknesses, various types of reinforcement have been developed and applied [11, 12].

Traditional steel reinforcement, such as rebar, has long been the standard in providing the tensile strength necessary to prevent cracking and improve the structural performance of concrete [13]. However, steel reinforcement is prone to corrosion, especially in aggressive environments, and its weight can pose challenges in some applications [14]. As a result, alternative reinforcement materials, such as fiber-reinforced polymers (FRPs), have gained prominence in recent years. FRPs, which include carbon fiber-reinforced polymers (CFRPs), glass fiber-reinforced polymers (GFRPs), and aramid fiber-reinforced polymers (AFRPs), offer several advantages over steel, including superior corrosion resistance [15, 16], a high strength-to-weight ratio, and ease of application in retrofitting projects. These materials are particularly effective in seismic retrofitting, where their ability to provide confinement and tensile reinforcement helps prevent premature failure, enhance ductility, and improve the overall earthquake resistance of structures [17]. Other types of reinforcement include textile-reinforced concrete (TRC), which integrates high-strength fibers into concrete matrices [18], and prestressed reinforcement, where steel or FRP tendons are tensioned to impart compressive stresses, further enhancing the structural capacity and reducing deflection. Together, these different types of reinforcement play a crucial role in improving the safety, durability, and performance of concrete structures, particularly in regions prone to seismic activity [19].

The foundational research on the application of FRPs in concrete confinement can be traced back to the pioneering work of Wolf and Miessler [20-22]. Their studies established the baseline understanding of how FRPs interact with concrete, providing the impetus for extensive subsequent research aimed at optimizing these interactions [23]. Over the past few decades, a substantial body of research has emerged, exploring the mechanical properties, durability, and effectiveness of various FRP materials, particularly carbon fiber-reinforced polymers (CFRPs), in strengthening concrete structures [4, 24]. The confinement provided by CFRP has been shown to significantly enhance both the compressive strength and ductility of concrete, primarily due to its ability to induce a three-dimensional compressive stress state within the concrete matrix [25, 26]. This confinement mechanism delays the onset of cracking and significantly mitigates the propagation of micro-cracks, thereby altering the failure mode of concrete from a brittle to a more ductile response [27, 28].

Extensive research efforts have focused predominantly on the effects of full FRP confinement, where the concrete column is entirely encased by the FRP material [29]. This method has been shown to yield significant improvements in key structural performance metrics, including load-carrying capacity, ductility, energy dissipation, and failure mode [30]. However, the practical application of full confinement is often limited by economic factors, access constraints, and architectural considerations [31]. Consequently, partial confinement methods have garnered increased attention as they offer a more resource-efficient alternative while still providing substantial performance benefits. Partial confinement typically involves the strategic application of FRP in discrete strips or bands, spaced at intervals along the length of the column, rather than a continuous wrap [32, 33]. This approach is particularly advantageous in scenarios where full wrapping is impractical or unnecessary.

Recent studies have investigated a variety of partial confinement configurations, such as horizontal strips, spiral bands, and grid patterns [34, 35]. These studies have provided valuable insights into how different confinement patterns and configurations influence the structural performance of concrete columns. Key findings indicate that the effectiveness of partial confinement is highly dependent on several factors, including the spacing of the FRP strips, the orientation of the fibers, and the overall geometry of the confinement pattern [36]. In particular, spiral confinement has shown promise in enhancing concrete's axial strength and ductility, with fewer issues related to debonding and void formation compared to other methods [37]. Nonetheless, while partial confinement methods offer notable advantages, the research remains relatively limited in scope, particularly when it comes to comparing their performance directly with full confinement techniques. Furthermore, existing design codes and stress-strain models have been primarily developed for fully confined concrete, with limited provisions or guidelines for partially confined structures. This gap in the current literature and design standards underscores the need for further research to develop and validate predictive models that accurately capture the behavior of partially confined concrete under various loading conditions.

The present study seeks to address these gaps by conducting a comprehensive investigation into the effects of partial CFRP confinement on concrete columns. Specifically, this research will examine two prevalent modes of partial confinement: horizontal strip confinement and spiral band confinement. The study will systematically compare the structural performance of columns subjected to these partial confinement methods with those of unconfined and fully confined columns. Key performance indicators, such as failure modes, stress-strain behavior, ultimate axial stress, and strain capacities, will be meticulously analyzed. The findings are expected to contribute to a deeper understanding of how partial CFRP confinement can be optimized to achieve maximum structural benefits while minimizing material usage and cost. Ultimately, the insights gained from this study will inform the development of more nuanced design guidelines and stress-strain models, thereby enhancing the practical application of FRP reinforcement in the retrofitting and strengthening of concrete columns in real-world scenarios.

2. Materials and Methods

The concrete mix was designed using the Dreux-Gorisse method, a well-established procedure in concrete mix design [38]. The particle size distribution of the aggregates, sands, and cement used in the mix was determined through particle size analysis tests, conducted in accordance with the NF EN 933-1 standard [39]. Table 1 provides a detailed overview of the mix design, including the proportions of each component, as well as the principal properties of the resulting concrete. This methodical approach ensures a well-graded mix that meets the specific requirements for both workability and strength.

Table 1. Mix proportions and characteristics of the concrete used

Component	Quantity
Cement (kg/m^3)	210
Water (kg/m^3)	115.5
Coarse aggregate 3/8 (kg/m^3)	218.68
Coarse aggregate 8/15 (kg/m^3)	977.06
Coarse Sand 0/3 (kg/m^3)	847.24
Water-to-Cement Ratio (W/C)	0.55
Compressive Strength, f_{co} (MPa)	21.42
Ultimate Strain, ε_{co} (%)	0.761

The mechanical properties of the carbon fiber-reinforced polymer (CFRP) composite, comprising both the fabric and the resin, were evaluated through standardized coupon testing.

Table 2. Properties of SikaWrap-230C/45 Fabric

Property	Value
Tensile Strength (MPa)	4.300
Tensile Modulus (MPa)	234.000
Ultimate Elongation (%)	1.8
Fiber Density (g/cm^3)	1.76
Fabric Thickness (mm)	0.13

Table 3. Properties of Sika Dur 330 Resin

Property	Value
Density (kg/l)	1.30
Tensile Strength (MPa)	> 30
Bond Strength to Concrete (MPa)	> 4
Elastic Modulus (MPa)	
- Flexural	3.800
- Tensile	4.50

Table 4. Mechanical Properties of CFRP Composite

Property	Value
Thickness of CFRP Composite t_f (per layer) (mm)	1
Elastic Modulus E_f (MPa)	34900
Tensile Strength f_{pr} (MPa)	480
Ultimate Strain ϵ_{fu}	2%

The results, detailed in Table 4, provide a comprehensive assessment of the composite's performance characteristics, including tensile strength, elasticity, and overall durability, crucial for understanding its behavior under various loading conditions. A total of cylindrical concrete specimens, each with a height of 320 mm and a diameter of 160 mm, were prepared and divided into eight distinct groups. Each configuration was tested three times to ensure statistical reliability. The confinement methods investigated included both full and partial confinement, employing horizontal and spiral bands. For partial confinement, the study evaluated parameters such as band spacing, the orientation of the bands relative to the horizontal, and the quantity of CFRP material used. In the experimental program, a consistent band width of 30 mm of unidirectional CFRP was used across all specimens, with the band spacing set at 30 mm, 45 mm, and 65 mm for both horizontal and spiral confinement methods. For specimens subjected to spiral partial confinement, additional reinforcement was applied at the specimen ends using a supplementary layer of unidirectional CFRP bands, each 20 mm wide, to improve end confinement and prevent premature failure. The labeling of the specimens followed a systematic convention: the first letter indicates the type of confinement (e.g., partial or full), the second letter specifies the confinement method (horizontal or spiral), the third

letter refers to the mode of confinement (e.g., uniform or partial), and the final numeral denotes the band spacing in millimeters. This standardized labeling ensured clear identification of each test configuration and its corresponding mechanical performance results.

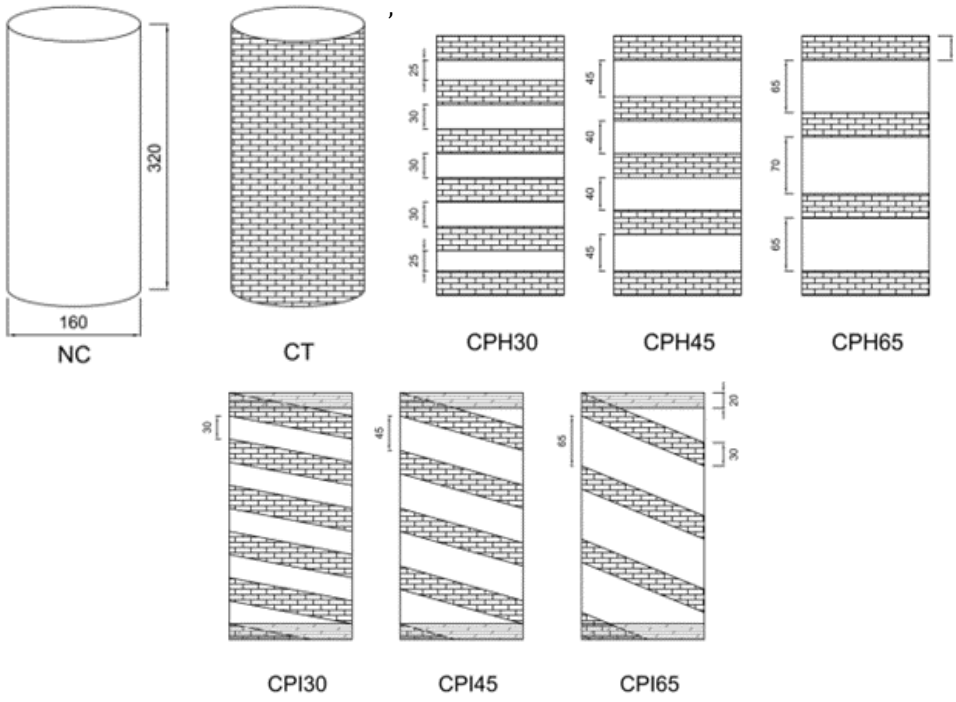

Fig. 1. Aspect of different confined configurations

For example, CPH45 denotes specimens partially confined with horizontal bands spaced 45 mm apart. Detailed confinement arrangements are illustrated in Figure 1. Compression tests were conducted using a universal testing machine (MCC8) with a capacity of 3000 kN, applying a controlled load increase rate of 0.5 MPa/s, as depicted in Figure 2. The positions of the bands on the specimens were marked using adhesive tape on the concrete surface (Figure 2). To ensure optimal contact between the load cell and the specimen, high-strength sulfur was used (Figure 2). Axial displacement measurements were recorded using three linear variable differential transformers (LVDTs) placed at mid-height (Figure 2). All confined specimens were overlapped by 150 mm according to the technical specifications of the SikaWrap-230C/45 fabric. They were cured at ambient laboratory conditions for 7 days to allow the epoxy resin to achieve full strength before testing. The abbreviations used to identify the specimen series are as follows:

- NC: Non-confined cylinders.
- CT: Cylinders fully confined with a single layer of CFRP.
- CP: Partially confined cylinders, where the second part of the code indicates either H for horizontal bands or I for spiral bands, and the third part specifies the spacing between bands (30 mm, 45 mm, or 65 mm). For instance, CPH45 refers to cylinders partially confined with horizontal bands spaced 45 mm apart.

Fig. 2. Methodology of CFRP application

3. Results and Discussion

3.1. Stress-Strain Behavior

Figure 3 presents the stress-strain behavior of all studied groups. Axial strains were determined using LVDTs, with the measurements obtained from three LVDTs placed at mid-height, as recommended by various researchers [40].

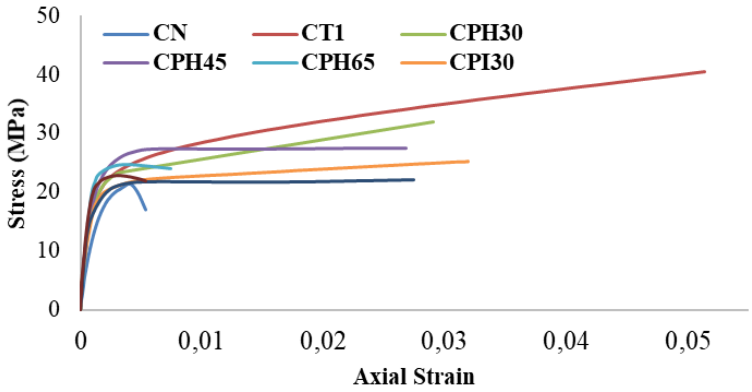

Fig. 3. Stress-Strain curves of all groups

Figure 3 displays the stress-strain curves for fully confined cylinders using CFRP composites. These curves reveal an initial ascending phase followed by a stress-softening branch. Conversely, the stress-strain behavior of partially confined concrete, shown in Figure 4, typically follows a bilinear pattern with hardening until failure (CFRP rupture). Initially, the curves exhibit linear behavior, dominated by the unconfined concrete's strength, indicating minimal activation of the CFRP confinement due to negligible lateral expansion. As the concrete experiences lateral expansion and increased axial strains, the response transitions to nonlinear. CFRP confinement becomes effective after the

unconfined concrete reaches its ultimate strength (fco= 21.42 MPa), resulting in additional cracking and a reduction in concrete stiffness.

For specimens with horizontal CFRP strips spaced 30 mm apart, the stress continued to rise linearly with a gradual slope until failure (f_{cc}= 32.03 MPa), as shown in Figure 4. At this point, the concrete was fully cracked, and CFRP confinement was fully engaged, leading to enhanced load capacity, increased compressive strength, and significantly improved ductility.

Specimens partially confined with horizontal CFRP strips spaced 45 mm apart exhibited a bilinear stress-strain response with significant ductility, maintaining a consistent slope until failure at 27.4 MPa, as illustrated in Figure 4. The final stress at failure was substantially higher than the unconfined concrete strength, indicating effective confinement.

For specimens with strips spaced 65 mm apart (Figure 4), the stress-strain curves displayed a descending branch characterized by stress softening up to failure. The concrete sustained a portion of the axial load after reaching a peak strength of 24.71 MPa, but the strength gradually decreased until failure occurred at 23.84 MPa, slightly above the unconfined concrete strength (f_{co} = 21.42 MPa). Therefore, the confinement level was still deemed adequate.

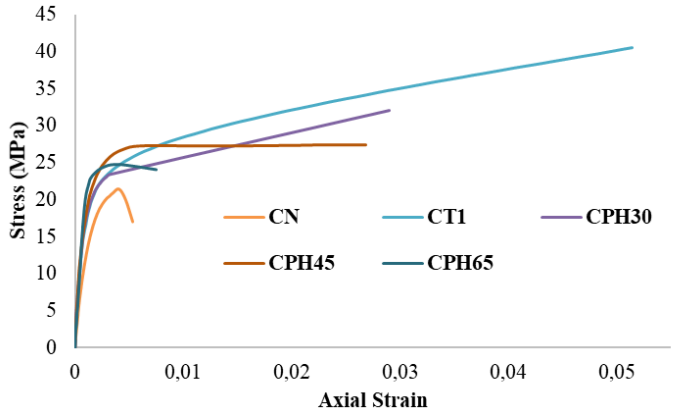

Fig. 4. Stress-Strain curves of horizontally confined groups

Figure 5 compares the stress-strain curves of partially confined cylinders with CFRP strips inclined at various angles to the horizontal. Each group has different spacings between the CFRP strips, resulting in different inclination angles, enabling a direct comparison between the series. As depicted in Figure 5, the stress-strain behavior of these specimens initially followed a linear path, similar to that of unconfined samples. For specimens with 30 mm and 45 mm spacings, the stress-strain curves exhibited a bilinear pattern with notable axial strain softening up to failure. The final stress at failure slightly exceeded the ultimate strength of the unconfined concrete.

For specimens with inclined CFRP strips spaced 65 mm apart (CPI65), the stress-strain curves displayed a short descending branch leading up to failure, with observable axial strain softening. These curves closely resemble those of specimens with horizontal CFRP strips spaced 65 mm apart (CPH65). Figures 3 to 5 demonstrate that the stress-strain curves for CFRP-confined concrete generally consist of two distinct segments, with the second segment either ascending or descending. In most specimens, the axial stresses increase monotonically until failure.

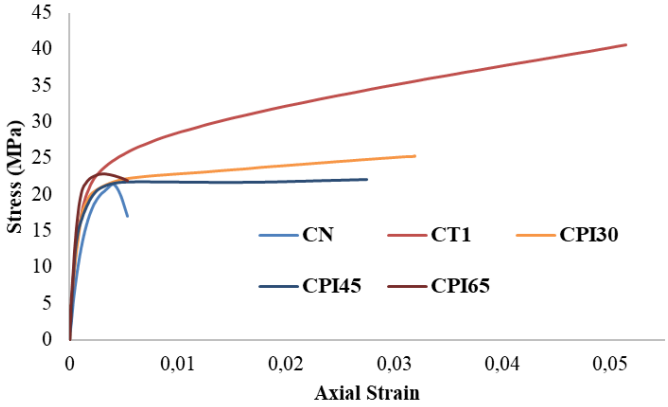

Fig. 5. Stress-Strain curves of spirally confined groups

However, only the stress-strain curves of the specimens with horizontal and inclined CFRP strips spaced 65 mm apart (CPH65 and CPI65) exhibit a descending branch. The relatively low volumetric ratios of CFRP applied in these two series are insufficient to produce a monotonically ascending stress-strain behavior. The volumetric ratio of CFRP is defined as:

$$\rho_f = \frac{A_f \pi D}{(\pi D^2/4)} = \frac{4 b_f n t_f}{DS} \quad (1)$$

Where: b_f, n_f, t_f represent the width of the FRP bands, the number of FRP layers, and the thickness of the FRP used for the confinement of the cylinder, respectively. D and S refers to the diameter and cross-sectional area of the column.

For specimens with a 65 mm spacing, the level of confinement approaches the threshold of inadequacy, leading to a reduced strength gain. In contrast, specimens with sufficient confinement, achieved through smaller spacings of 30 mm and 45 mm, exhibit significantly enhanced compressive strength and ultimate axial strain due to the more effective confinement.

3.2. Failure Mode

The groups exhibited distinct failure modes, as illustrated in Figure 6:

- Non-confined cylinders (NC): Failure initiation occurred through inclined cracking within the concrete, ultimately leading to concrete crushing as the primary failure mode (Figure 6-a).
- Fully confined cylinders (CT): The CFRP failed locally at mid-height due to concentrated lateral confinement, resulting in a sudden CFRP rupture accompanied by a significant explosion (Figure 6-b).
- Partially confined cylinders with 65 mm spacing (CPH65 and CPI65): These specimens predominantly failed through concrete crushing. Cracks formed between adjacent CFRP strips as the axial stress approached the strength of unconfined concrete, with the failure mode being characterized by diagonal shear cracking (Figures 6-c and 6-d).
- Partially confined cylinders with horizontal or spiral CFRP strips (CPH30, CPI30, CPH45, and CPI45): These specimens experienced CFRP strip rupture at mid-height due to tensile stress. The failure was marked by the disintegration of the concrete core, resulting in a conical cracking mode (Figures 6-e to 6-h).

- Cylinders subjected to compression: Failure occurred suddenly and explosively following CFRP composite rupture. The concrete adhered to the CFRP composite, indicating strong adhesion between the two materials (Figure 6). Post-explosion, intact CFRP strips were observed in several specimens.

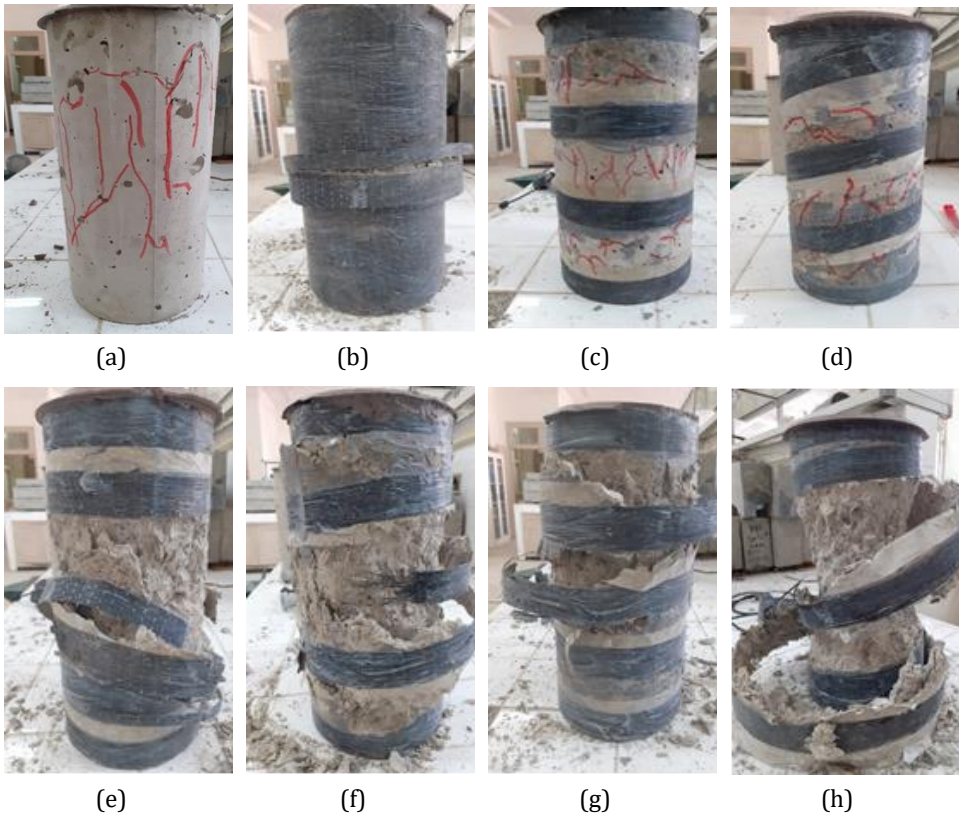

(a) (b) (c) (d)

(e) (f) (g) (h)

Fig. 6. Failure modes of specimens

Additionally, CFRP rupture did not occur at the cylinder ends due to the increased friction from the loading platens near both ends, as noted by Teng et al. (2015b). This expanded explanation provides a clearer understanding of the failure mechanisms across different confinement scenarios, highlighting the influence of CFRP strip spacing and orientation on the overall structural behavior. The observations underscore the critical role of adequate confinement in enhancing the load-bearing capacity and failure resistance of concrete cylinders.

3.3. Effect of Strip Spacing on Partial Confinement

Figure 7 provides a summary of the average compressive strength values and axial strains for all studied samples. It is evident that both partial and full CFRP confinement significantly enhance the ultimate compressive strength of the specimens compared to unconfined samples. The fully CFRP-confined cylinders demonstrated the highest strength improvement, with an increase of 89.36%. Among the partially confined specimens, those with horizontal CFRP strips spaced 30 mm apart showed the most substantial strength improvement, with a 49.53% increase over unconfined samples. This result indicates that the compressive strength of partially confined CFRP samples is approximately 21.03% lower than that of fully confined samples. However, this difference is relatively minor

considering the material savings achieved. Additionally, this configuration exhibited a 610.78% increase in axial strain compared to unconfined samples, although this is 43.56% lower than the axial strain observed in fully confined CFRP specimens. The effect of increased horizontal spacing on maximum axial strain was also apparent. Specimens with 45 mm and 65 mm spacing showed increases in displacement of approximately 556.48% and 106.40%, respectively.

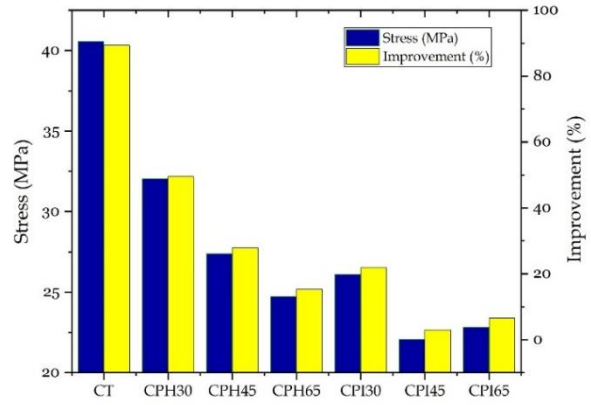

(a)

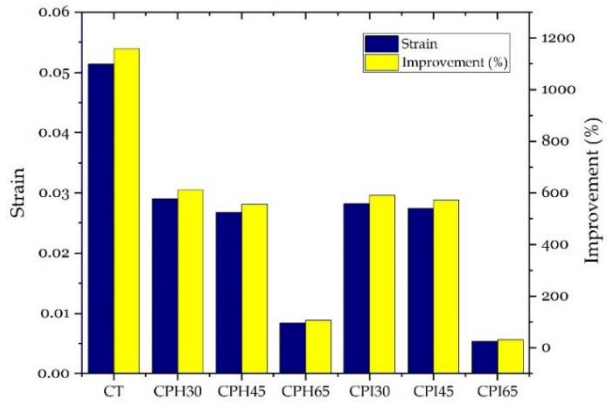

(b)

Fig. 7. Summary of experimental results compared to unconfined cylinders

For cylinders confined with spiral CFRP strips, the compressive strength results were more nuanced. The strength increased by 3.03% with 45 mm spacing and by 6.58% with 65 mm spacing. Although these values were lower compared to those with horizontal CFRP strips, a maximum strength increase of 21.90% over unconfined concrete was observed. The relationship between spiral spacing and ultimate axial strain was also evident, with displacement increasing as the spacing between spiral bands decreased. Specifically, axial strains increased by 591.42% at 30 mm spacing, 572.67% at 45 mm, and 30.47% at 65 mm spacing. Unconfined concrete had an axial strain of 0.00408, whereas the highest axial strains recorded were 0.0514 for fully confined specimens and 0.029 for all partial confinement configurations. This analysis underscores the significant impact of CFRP confinement on enhancing the compressive strength and axial strain capacity of concrete specimens, with the degree of improvement closely related to the confinement

configuration and the spacing of the CFRP strips. In addition to their impact on compressive strength, CFRP confinement techniques can also influence the bending and shear performance of concrete elements. Research has shown that CFRP reinforcement not only improves the flexural capacity of beams but also enhances shear strength, particularly in cases where transverse reinforcement is insufficient. These improvements are attributed to the ability of CFRPs to provide lateral confinement, reduce crack propagation, and enhance the overall ductility of concrete members. Thus, incorporating CFRP in both bending and shear applications presents a comprehensive solution for strengthening concrete structures.

3.4. Comparative Analysis of Strength Performance Between Full and Partial CFRP Confinement

Figure 8 presents a detailed comparison of the strength enhancements achieved through full versus partial CFRP confinement. The analysis reveals a strength differential of -21.03% between specimens confined with horizontal CFRP strips spaced at 30 mm and those fully confined with CFRP, where the composite material used in partial confinement represents less than half of the amount employed in full confinement. Despite the reduced material usage, the partially confined specimens exhibited a significant level of effectiveness in enhancing the compressive strength of the concrete cylinders.

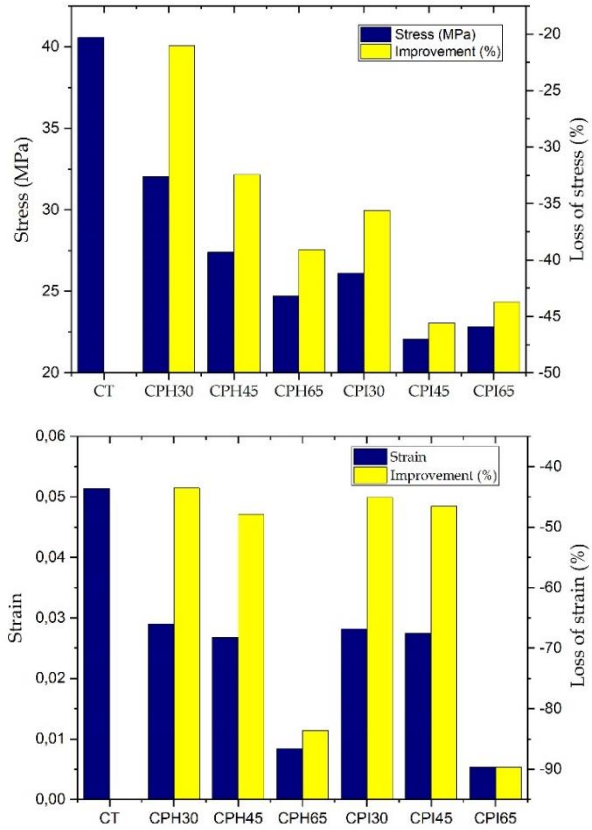

Fig. 8. Summary of experimental results relative to fully confined cylinders

The results indicate that the CPI45 specimen, with a strength improvement -45.59% lower than fully confined concrete, exhibited the least favorable performance among the partially confined samples. Notably, partial confinement using horizontal CFRP strips consistently outperformed spiral CFRP strip configurations in terms of strength enhancement. These findings underscore the efficacy of partial CFRP confinement, particularly with horizontal strips, in achieving substantial strength gains while optimizing material efficiency. The observed performance suggests that partial confinement can be a viable alternative to full confinement, offering a balance between structural enhancement and material economy.

3.5. Numerical Verification

Tables 5 and 6 present the ($\frac{\Delta f_{cc}}{f_{cc,exp}}$) between the theoretical maximum compressive strength $f_{cc,thé}$ and the experimental maximum compressive strength $f_{cc,exp}$for three design codes and three models of CFRP-confined concrete under axial compression ($\Delta f_{cc} = f_{cc,thé} - f_{cc,exp}$). Most predictions related to the compressive strength of CFRP-confined concrete appeared conservative compared to the experimental strength, with prediction results generally varying between 19% and -2% for horizontal partial confinement, though predictions for full confinement were somewhat less accurate. Despite these results, the models were still able to provide the best prediction for horizontal partial confinement, where the prediction values were closely aligned, ranging between -2% and 4%, with a maximum difference of 1 MPa. However, predictions for fully CFRP-confined concrete were overestimated by 20% when using the FIB model [41] .

Although the ACI code [42] does not account for partial confinement factors and fiber orientation reduction, the CFRP horizontal and spiral strip positions were considered using the k_e coefficient from the FIB model. The predicted confinement strength for most specimens remained within the range of -16% to 19%. Generally, the values predicted using the ACI code were very close to those of the CSA S806 code [43] and higher than those predicted by the FIB code for most samples. Nevertheless, the FIB model provided a more accurate prediction of confinement strength, particularly for partially CFRP-confined concrete, compared to the CSA S806 and ACI codes.

Table 5. Verification of design codes against experimental results

	b_f (mm)	s (mm)	Experimental	FIB Standard		CSA S806 standard		ACI Standard	
			$f_{cc,exp}$ (MPa)	$f_{cc,thé}$ (MPa)	$\frac{\Delta f_{cc}}{f_{cc,exp}}$	$f_{cc,thé}$ (MPa)	$\frac{\Delta f_{cc}}{f_{cc,exp}}$	$f_{cc,thé}$ (MPa)	$\frac{\Delta f_{cc}}{f_{cc,exp}}$
CT	/	/	40.56	48.83	20%	33.70	-17%	44.82	11%
CPH30	30	30	32.03	32.83	2%	31.36	-2%	40.64	27%
CPH45	30	45	27.4	28.50	4%	30.25	10%	38.70	41%
CPH65	30	65	24.71	24.23	-2%	28.83	17%	36.28	47%
CPI30	30	30	26.11	35.73	37%	33.65	29%	44.76	71%
CPI45	30	45	22.07	32.41	47%	33.65	52%	44.76	71%
CPI65	30	65	22.83	29.27	28%	33.65	47%	44.76	71%

The models proposed by Pellegrino et al [44] and Wang et al. [45] recommend using the k_e coefficient from FIB to account for the effect of strip spacing. These two models provide reasonable predictions for partially CFRP-confined concrete with horizontal strips, with the ratio between experimental and theoretical results ranging from 0% to 10% and 1% to 8%, respectively, with a maximum difference of 4 MPa and 2 MPa for the Pellegrino & Modena (2010) and Wang et al. [45] models, respectively. However, the stress-strain

model for CFRP-confined concrete by Guo et al. [46] did not yield accurate predictions except for the case of full confinement. This model significantly overestimated the ultimate compressive strength of partially CFRP-confined concrete compared to experimental data. Although FIB differentiates the k_e coefficient for horizontal and spiral CFRP strip confinement, the difference in values for spiral strips was too minor. Considering the spiral strip spacing, the calculated k_e coefficient remained approximately equal to 1 regardless of the strip spacing. Consequently, both the FIB and other codes and models have evidently overestimated the ultimate axial stress.

Table 6. Verification of stress-strain models against experimental results

	b_f (mm)	S (mm)	Experimental	Pellegrino et al.		Wang *et al.*,		Guo *et al.*	
			$f_{cc,exp}$ (MPa)	$f_{cc,the}$ (MPa)	$\frac{\Delta f_{cc}}{f_{cc,exp}}$	$f_{cc,the}$ (MPa)	$\frac{\Delta f_{cc}}{f_{cc,exp}}$	$f_{cc,the}$ (MPa)	$\frac{\Delta f_{cc}}{f_{cc,exp}}$
CT	/	/	40.56	54.16	34%	47.96	18%	38.45	-5%
CPH30	30	30	32.03	28.80	-10%	32.32	1%	35.11	10%
CPH45	30	45	27.4	26.47	-3%	29.26	7%	33.57	23%
CPH65	30	65	24.71	24.66	0%	26.74	8%	31.64	28%
CPI30	30	30	26.11	30.64	17%	34.64	33%	38.38	47%
CPI45	30	45	22.07	28.55	29%	32.00	45%	38.38	74%
CPI65	30	65	22.83	26.85	18%	29.77	30%	38.38	68%

In conclusion, while the safety benefits of CFRP confinement in enhancing the structural performance of concrete are well-documented, it is equally important to consider the economic aspect. The initial cost of CFRP materials is typically higher than that of conventional reinforcement methods. However, the long-term advantages associated with CFRP, such as reduced maintenance requirements, extended service life, and the ability to retrofit existing structures without significant downtime, can effectively offset these initial costs. Consequently, when evaluating CFRP as a strengthening solution, it is crucial to strike a careful balance between safety and cost-effectiveness. This comprehensive approach ensures optimized decision-making in practical applications, ultimately leading to more sustainable and resilient structural solutions. By acknowledging both the immediate financial implications and the broader benefits of using CFRP, stakeholders can make informed choices that enhance the overall integrity and longevity of concrete structures.

4. Conclusion

- This research undertook an in-depth examination of the performance and predictive accuracy of various design codes and stress-strain models for CFRP-confined concrete. By evaluating different types of CFRP confinement—full, horizontal, and spiral—along with assessing the effectiveness of multiple design codes and models, the study aimed to provide a clearer understanding of how these factors influence concrete strength and axial strain capacity. The findings result shows:
- Full CFRP Confinement: Demonstrated a substantial improvement in compressive strength, with an increase of 89.36% compared to unconfined concrete. This type of confinement provided the highest enhancement in concrete strength and axial strain capacity.
- Horizontal CFRP Strips: Particularly effective, with specimens featuring strips spaced 30 mm apart showing a 49.53% increase in compressive strength. This

configuration also exhibited a 610.78% increase in axial strain compared to unconfined samples, although this was 43.56% lower than fully confined specimens.

- Spiral CFRP Strips: Less effective compared to horizontal strips. While the compressive strength increased by 21.90% over unconfined concrete, the axial strain improvements were less pronounced, with an increase of 591.42% at 30 mm spacing, 572.67% at 45 mm, and 30.47% at 65 mm spacing.
- The FIB (2001) model was effective for horizontal CFRP confinements but overestimated stress for spiral confinements, while the ACI (2017) code provided reasonable predictions with deviations between -16% and 19%. Models by Pellegrino & Modena (2010) and Wang et al. (2018) accurately predicted horizontal CFRP strip performance, with deviations of up to 10%, but struggled with spiral confinements. The Guo et al. (2019) model significantly overestimated strength for partially CFRP-confined specimens, with discrepancies up to 45.59%.
- In conclusion, the findings from this study offer valuable insights for decision-makers in the field of structural engineering and construction. The demonstrated effectiveness of fully and horizontally CFRP-confined concrete, along with the varying performance of spiral configurations, provides a clear basis for selecting the most appropriate confinement strategy depending on the specific structural requirements. Furthermore, the analysis of predictive models and design codes, such as FIB (2001), ACI (2017), and models by Pellegrino et al., Wang et al., and Guo et al., underscores the need for refinements in these tools to improve accuracy. Decision-makers can use this research to enhance construction practices by adopting CFRP confinement strategies that optimize strength and strain improvements, while also aligning with reliable predictive models. This, in turn, will contribute to more efficient and resilient concrete structures, ensuring better performance and longevity in civil engineering projects.

This study opens new avenues for enhancing CFRP confinement techniques in concrete, suggesting that more accurate predictive models could be developed, particularly for partial confinements and spiral configurations. The findings also highlight the need to revise and refine current design codes to more accurately reflect the actual behavior of CFRP-confined concrete, especially in applications requiring high strength and durability. Future research could focus on exploring the interaction between different confinement types and optimizing the use of composite materials to maximize both structural efficiency and cost-effectiveness.

Acknowledgments

The authors acknowledge the support from the Directorate-General for Scientific Research and Technological Development (DGRSDT-Algeria). The authors are grateful to Merdas Abdelghani (Department of Civil Engineering, University of Ferhat Abbas, Sétif, Algeria) for their help to conduct the experimental program at Emerging Materials Research Unit (EMRU).

Appendix

Model	Stress	Strain
FIB standard [41]	$f_{cc} = f_{co}\left(0.2 + 3\sqrt{\frac{f_l}{f_{co}}}\right)$	$\varepsilon_{cu} = \varepsilon_{co}\left(2 + 1.25\frac{E_c}{f_{co}}\varepsilon_{fe}\sqrt{\frac{f_l}{f_{co}}}\right)$
CSA S806 Standard [43]	$f_{cc} = 0.85f_{co} + k_l k_c f_l$	/
ACI Standard [42]	$f_{cc} = f_{co} + 3.1\kappa_a f_l$	$\varepsilon_{cu} = \varepsilon_{co}\left[1.5 + 12\kappa_b\frac{f_l}{f_{co}}\left(\frac{\varepsilon_{fe}}{\varepsilon_{co}}\right)^{0.45}\right] \leq 0.01$
Pellegrino et al. [44]	$\frac{f_{cu}}{f_{co}} = 1 + k_1\frac{P_u}{f_{co}}$	$\frac{\varepsilon_{cu}}{\varepsilon_{co}} = 2 + B(\frac{P_u}{f_{co}})$
Wang et al., [45]	$\frac{f_{cc}}{f_{co}} = 1 + 3.3k_e\frac{f_l}{f_{co}}$	$\frac{\varepsilon_{cu}}{\varepsilon_{co}} = 1.75 + 12\left(\frac{f_l}{f_{co}}\right)\left(\frac{\varepsilon_{h,rup}}{\varepsilon_{co}}\right)^{0.45}$
Guo et al., [46]	$\frac{f_{cc}}{f_{co}} = 1 + 2(\rho_{Ke} - 0.01)\rho_\varepsilon$	$\frac{\varepsilon_{cu}}{\varepsilon_{co}} = 1.75 + 5.5\rho_{Ke}^{0.8}\rho_\varepsilon^{1.45}$

F_{cc}: Compressive strength of CFRP-confined concrete, F_{co}: Compressive strength of unconfined concrete, F_l: Lateral confinement stress provided by the CFRP, k_e Efficiency factor for the confinement type, *S:* Spacing between confinement bands, *D:* Diameter of the concrete cylinder, ϵ_{cu} : Ultimate strain of CFRP-confined concrete, ϵ_{co} : Ultimate strain of unconfined concrete, E_c *:* Modulus of elasticity of concrete, ϵ_{fl}: Effective strain in the CFRP material, *Kl*: Confinement factor related to the lateral confinement stress, *Kc*: Geometric factor for the section shape, *Kα*: Coefficient related to the axial confinement stress, *Kb*: Coefficient related to the deformation, $\boldsymbol{\rho\kappa e}$: Confinement stiffness ratio, $\boldsymbol{\rho\varepsilon}$: Confinement strain ratio, $\boldsymbol{\varepsilon h,rup}$: Ultimate strain of the CFRP jacket at rupture, $\boldsymbol{\varepsilon co}$: Strain of unconfined concrete under compression corresponding to $\boldsymbol{fc}$ or the applied compression load

References

[1] Hao H, Bi K, Chen W, Pham TM, Li J. Towards next generation design of sustainable, durable, multi-hazard resistant, resilient, and smart civil engineering structures. Eng Struct. 2023;277:115477. https://doi.org/10.1016/j.engstruct.2022.115477

[2] Singh P, Singh S, Ojha R, Tiwari P, Khan S, Kumar R, et al. Characterization of wear of FRP composites: A review. Mater Today Proc. 2022;64:1357-61. https://doi.org/10.1016/j.matpr.2022.04.236

[3] Siddika A, Al Mamun MA, Ferdous W, Alyousef R. Performances, challenges and opportunities in strengthening reinforced concrete structures by using FRPs-A state-of-the-art review. Eng Fail Anal. 2020;111:104480. https://doi.org/10.1016/j.engfailanal.2020.104480

[4] Ortiz JD, Khedmatgozar Dolati SS, Malla P, Nanni A, Mehrabi A. FRP-reinforced/strengthened concrete: State-of-the-art review on durability and mechanical effects. Materials. 2023;16(5):1990. https://doi.org/10.3390/ma16051990

[5] İnce O. Structural damage assessment of reinforced concrete buildings in Adıyaman after Kahramanmaraş (Türkiye) Earthquakes on 6 February 2023. Eng Fail Anal. 2024;156:107799. https://doi.org/10.1016/j.engfailanal.2023.107799

[6] Işık E, Avcil F, İzol R, Büyüksaraç A, Bilgin H, Harirchian E, et al. Field reconnaissance and earthquake vulnerability of the RC buildings in Adıyaman during 2023 Türkiye Earthquakes. Appl Sci. 2024;14(7):2860. https://doi.org/10.3390/app14072860
[7] Akar F, Işık E, Avcil F, Büyüksaraç A, Arkan E, İzol R. Geotechnical and structural damages caused by the 2023 Kahramanmaraş Earthquakes in Gölbaşı (Adıyaman). Appl Sci. 2024;14(5):2165. https://doi.org/10.3390/app14052165
[8] Ivanov ML, Chow W-K. Structural damage observed in reinforced concrete buildings in Adıyaman during the 2023 Türkiye Kahramanmaraş Earthquakes. Struct. 2023:105578. https://doi.org/10.1016/j.istruc.2023.105578
[9] Avcil F, Işık E, İzol R, Büyüksaraç A, Arkan E, Arslan MH, et al. Effects of the February 6, 2023, Kahramanmaraş earthquake on structures in Kahramanmaraş city. Nat Hazards. 2024;120(3):2953-91. https://doi.org/10.1007/s11069-023-06314-1
[10] Abdesselam A, Merdas A, Fiorio B, Chikh N-E. Experimental and numerical study on RC beams strengthened by NSM using CFRP reinforcements. Period Polytech Civ Eng. 2023;67(4):1214-33. https://doi.org/10.3311/PPci.21309
[11] Merdas A, Fiorio B, Chikh N-E. Study of the adhesion of composite strips and rods to concrete by bending (the beam test). C R Mec. 2011;339(12):796-804. https://doi.org/10.1016/j.crme.2011.10.002
[12] Merdas A, Fiorio B, Chikh N-E. Aspects of bond behavior for concrete beam strengthened with carbon fibers reinforced polymers-near surface mounted. J Reinf Plast Compos. 2015;34(6):463-78. https://doi.org/10.1177/0731684415573814
[13] Mesbah H-A, Benzaid R. Damage-based stress-strain model of RC cylinders wrapped with CFRP composites. Adv Constr Mater. 2017;5(5):539.
[14] Benzaid R, Chikh N-E, Mesbah H. Study of the compressive behavior of short concrete columns confined by fiber reinforced composite. Arab J Sci Eng. 2009;34(1B):15-26.
[15] Benzaid R, Mesbah H-A. The confinement of concrete in compression using CFRP composites-effective design equations. J Civ Eng Manag. 2014;20(5):632-48. https://doi.org/10.3846/13923730.2013.801911
[16] Mesbah H-A, Benzaid R, Benmokrane B. Evaluation of bond strength of FRP reinforcing rods in concrete and FE modelling. Int J Civ Eng Constr Sci. 2017;4(3):21-41.
[17] Benzaid R, Mesbah H, Chikh N-E. FRP-confined concrete cylinders: axial compression experiments and strength model. J Reinf Plast Compos. 2010;29(16):2469-88. https://doi.org/10.1177/0731684409355199
[18] Venigalla SG, Nabilah AB, Mohd Nasir NA, Safiee NA, Abd Aziz FNA. Textile-reinforced concrete as a structural member: a review. Buildings. 2022;12(4):474. https://doi.org/10.3390/buildings12040474
[19] Huang Y, Grünewald S, Schlangen E, Luković M. Strengthening of concrete structures with ultra high performance fiber reinforced concrete (UHPFRC): A critical review. Constr Build Mater. 2022;336:127398. https://doi.org/10.1016/j.conbuildmat.2022.127398
[20] Douadi A, Merdas A, Sadowski Ł. The bond of near-surface mounted reinforcement to low-strength concrete. J Adhes Sci Technol. 2019;33(12):1320-36. https://doi.org/10.1080/01694243.2019.1592944
[21] Boutlikht M, Lahbari N, Hebbache K, Tabchouche S. The assessment of strips arrangement effect on the performance of strengthened reinforced concrete beams. J Adhes Sci Technol. 2022;36(14):1510-27. https://doi.org/10.1080/01694243.2021.1977475
[22] Karouche A, Hebbache K, Belebchouche C, Lahbari N, Kessal O, Czarnecki S. External confined concrete cylinders behavior under axial compression using CFRP wrapping. Materials. 2022;15(22):8232. https://doi.org/10.3390/ma15228232
[23] Bisby LA. Fire behaviour of fibre-reinforced polymer (FRP) reinforced or confined concrete [dissertation]. Queen's University Kingston; 2003.

[24] Amran YM, Alyousef R, Rashid RS, Alabduljabbar H, Hung C-C. Properties and applications of FRP in strengthening RC structures: A review. Struct. 2018:208-38. https://doi.org/10.1016/j.istruc.2018.09.008
[25] Bai Y-L, Dai J-G, Teng J. Cyclic compressive behavior of concrete confined with large rupture strain FRP composites. J Compos Constr. 2014;18(1):04013025. https://doi.org/10.1061/(ASCE)CC.1943-5614.0000386
[26] Wang Y, Cai G, Larbi AS, Waldmann D, Tsavdaridis KD, Ran J. Monotonic axial compressive behaviour and confinement mechanism of square CFRP-steel tube confined concrete. Eng Struct. 2020;217:110802. https://doi.org/10.1016/j.engstruct.2020.110802
[27] Bains A. Numerical modelling of micro and macro cracking in plain and fibre-reinforced cementitious composites [dissertation]. Cardiff University; 2021.
[28] Le LA, Nguyen GD, Bui HH, Sheikh AH, Kotousov A. Incorporation of micro-cracking and fibre bridging mechanisms in constitutive modelling of fibre reinforced concrete. J Mech Phys Solids. 2019;133:103732. https://doi.org/10.1016/j.jmps.2019.103732
[29] Pham TM, Youssed J, Hadi MN, Tran TM. Effect of different FRP wrapping arrangements on the confinement mechanism. Procedia Eng. 2016;142:307-13. https://doi.org/10.1016/j.proeng.2016.02.051
[30] Magliaro J, Altenhof W, Alpas AT. A review of advanced materials, structures and deformation modes for adaptive energy dissipation and structural crashworthiness. Thin-Walled Struct. 2022;180:109808. https://doi.org/10.1016/j.tws.2022.109808
[31] Goel RK, Singh B, Zhao J. Underground infrastructures: planning, design, and construction. Butterworth-Heinemann; 2012. https://doi.org/10.1016/B978-0-12-397168-5.00007-9
[32] Kalfat R, Gadd J, Al-Mahaidi R, Smith ST. An efficiency framework for anchorage devices used to enhance the performance of FRP strengthened RC members. Constr Build Mater. 2018;191:354-75. https://doi.org/10.1016/j.conbuildmat.2018.10.022
[33] Lin S, Zhao Y-G, Li J. An improved wrapping scheme of axially loaded fiber-reinforced polymer confined concrete columns. Compos Struct. 2019;226:111242. https://doi.org/10.1016/j.compstruct.2019.111242
[34] Azhand A. Three-dimensional nonlinear waves under spatial confinement [dissertation]. 2016.
[35] Tejada ODT. Experimental assessment of FRP-confined concrete columns with damaged jackets [dissertation]. Queen's University; 2021.
[36] Liao J, Zeng J-J, Jiang C, Li J-X, Yuan J-S. Stress-strain behavior and design-oriented model for FRP spiral strip-confined concrete. Compos Struct. 2022;293:115747. https://doi.org/10.1016/j.compstruct.2022.115747
[37] Deogekar PS, Andrawes B. Hybrid confinement of high strength concrete using shape memory alloys and fiber-reinforced polymers. J Struct Integr Maint. 2018;3(1):22-32. https://doi.org/10.1080/24705314.2018.1426172
[38] Dreux G, Festa J. Nouveau guide du béton et de ses constitutants. Eyrolles; 1998.
[39] N.E. 933-1. Essais pour déterminer les caractéristiques géométriques des granulats - Partie 1 : détermination de la granularité - Analyse granulométrique par tamisage. 2012:19.
[40] Chen G, He Y, Jiang T, Lin CJ. Behavior of CFRP-confined recycled aggregate concrete under axial compression. Build Mater. 2016;111:85-97. https://doi.org/10.1016/j.conbuildmat.2016.01.054
[41] Triantafillou T, Matthys S, Audenaert K, Balázs G, Blaschko M, Blontrock H, et al. Externally bonded FRP reinforcement for RC structures. Int Fed Struct Concr. 2001. https://doi.org/10.35789/fib.BULL.0014
[42] Silva P, Kanitkar R. ACI 440.2 R and the new seismic strengthening guidelines using FRP. Spec Publ. 2018;327:20.1-20.16.

[43] Canadian Standards Association. Design and construction of building structures with fibre-reinforced polymers. 2012.
[44] Pellegrino C, Modena CJ. Analytical model for FRP confinement of concrete columns with and without internal steel reinforcement. J Compos Constr. 2010;14(6):693-705. https://doi.org/10.1061/(ASCE)CC.1943-5614.0000127
[45] Wang W, Martin PR, Sheikh MN, Hadi MNJ. Eccentrically loaded FRP confined concrete with different wrapping schemes. J Compos Constr. 2018;22(6):04018056. https://doi.org/10.1061/(ASCE)CC.1943-5614.0000898
[46] Guo Y-C, Gao W-Y, Zeng J-J, Duan Z-J, Ni X-Y, Peng KD. Compressive behavior of FRP ring-confined concrete in circular columns: Effects of specimen size and a new design-oriented stress-strain model. Constr Build Mater. 2019;201:350-68. https://doi.org/10.1016/j.conbuildmat.2018.12.183